Electronic Supplementary Material (ESI) for Polymer Chemistry.


# Supporting Information for:

## Synthesis, characterisation and Pickering emulsifier performance of poly(stearyl methacrylate)-poly(*N*-2-(methacryloyloxy)ethyl pyrrolidone) diblock copolymer nano-objects via RAFT dispersion polymerisation in *n*-dodecane

Victoria J. Cunningham and Steven P. Armes*

*Department of Chemistry, University of Sheffield, Brook Hill, Sheffield, South Yorkshire, S3 7HF, UK.*

Osama M. Musa

*Ashland Specialty Ingredients, 1005 US 202/206, Bridgewater, NJ 08807, USA.*

**Synthesis of $PSMA_{14}$-$PBzMA_{95}$ via RAFT dispersion polymerisation of SMA**

$PSMA_{14}$ macro-CTA (0.2201 g), BzMA (0.7728 g, 4.386 mmol), T21s (2.37 mg, 26 µmol; dissolved at 10% v/v in *n*-dodecane; CTA/T21s molar ratio = 4.0) were dissolved in *n*-dodecane (4.13.9713 g, 10% w/w) in a 25 ml round-bottomed flask. The reaction mixture was sealed and purged with nitrogen for 30 min, prior to immersion in an oil bath set at 90 °C. Aliquots were taken every 10 min for the first hour and analysed by $^1$H NMR analysis. A final conversion of 95% was achieved after 6 h. The resulting copolymer was analysed using 3:1 chloroform/methanol GPC ($M_n$ = 23,800 g mol$^{-1}$, $M_w/M_n$ = 1.10 vs. PMMA standards). DLS studies on a 0.20% w/w copolymer dispersion indicated an intensity-average particle diameter of 181 nm (DLS polydispersity, PDI = 0.260). TEM studies confirmed a worm-like morphology at 95 % conversion.

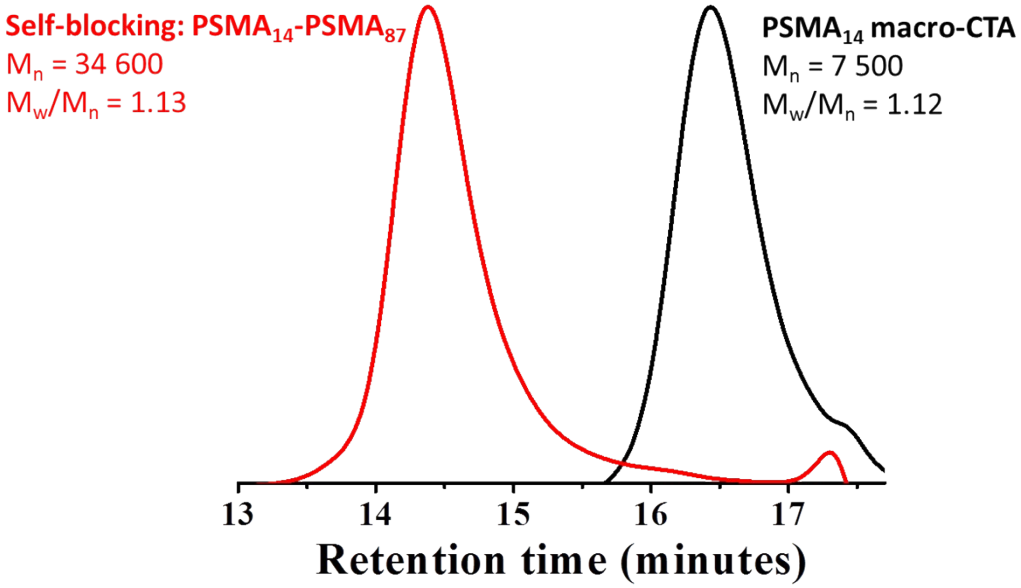


**Figure S1.** 3:1 Chloroform/methanol GPC curves obtained for the initial $PSMA_{14}$ macro-CTA and the corresponding $PSMA_{14}$-$PSMA_{87}$ after a 'self-blocking' chain extension experiment at 90 °C.

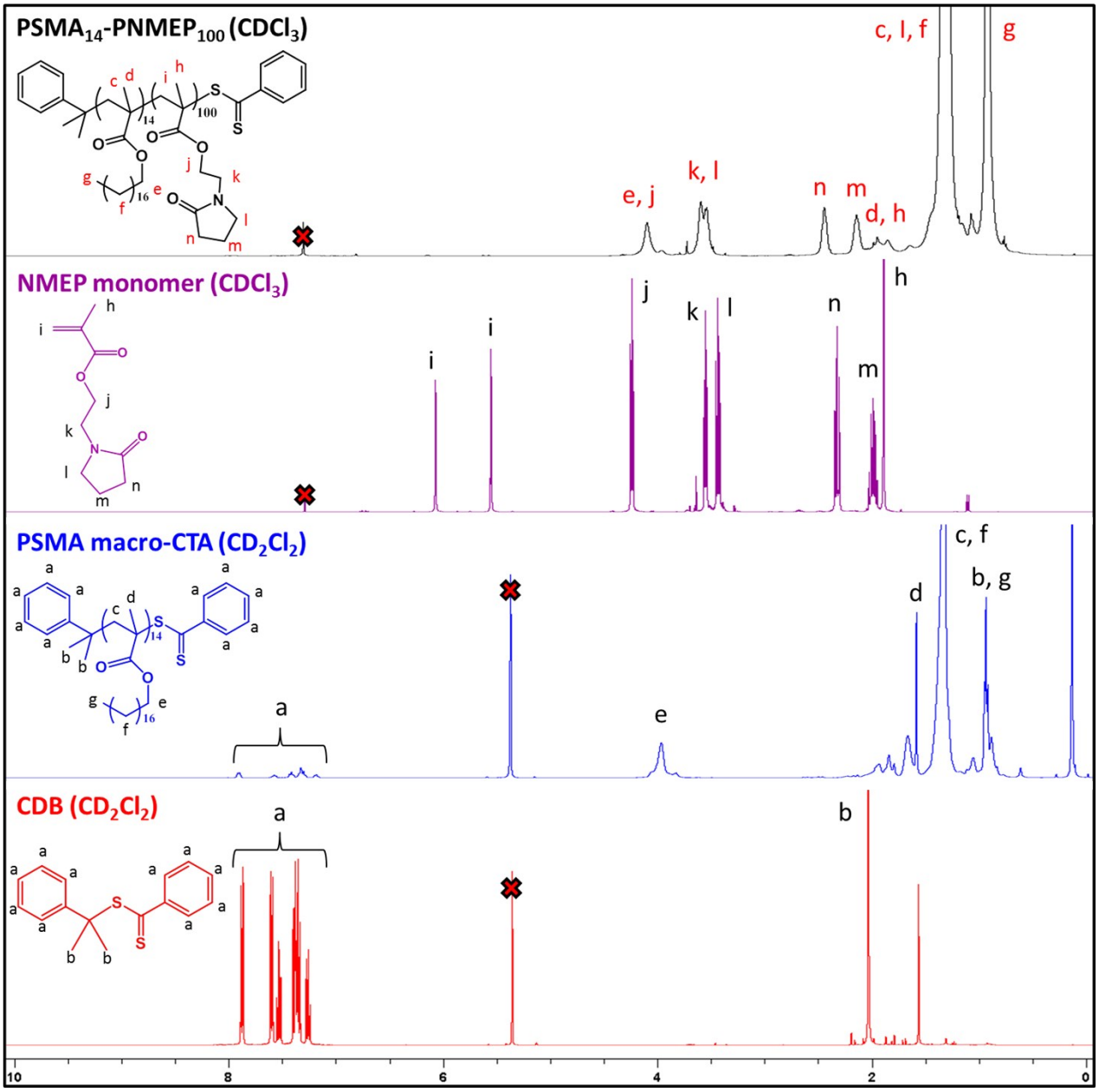


**Figure S2.** Assigned $^{1}H$ NMR spectra obtained for the CDB RAFT agent, a $PSMA_{14}$ macro-CTA, the NMEP monomer and a $PSMA_{14}$-$PNMEP_{100}$ diblock copolymer.

.

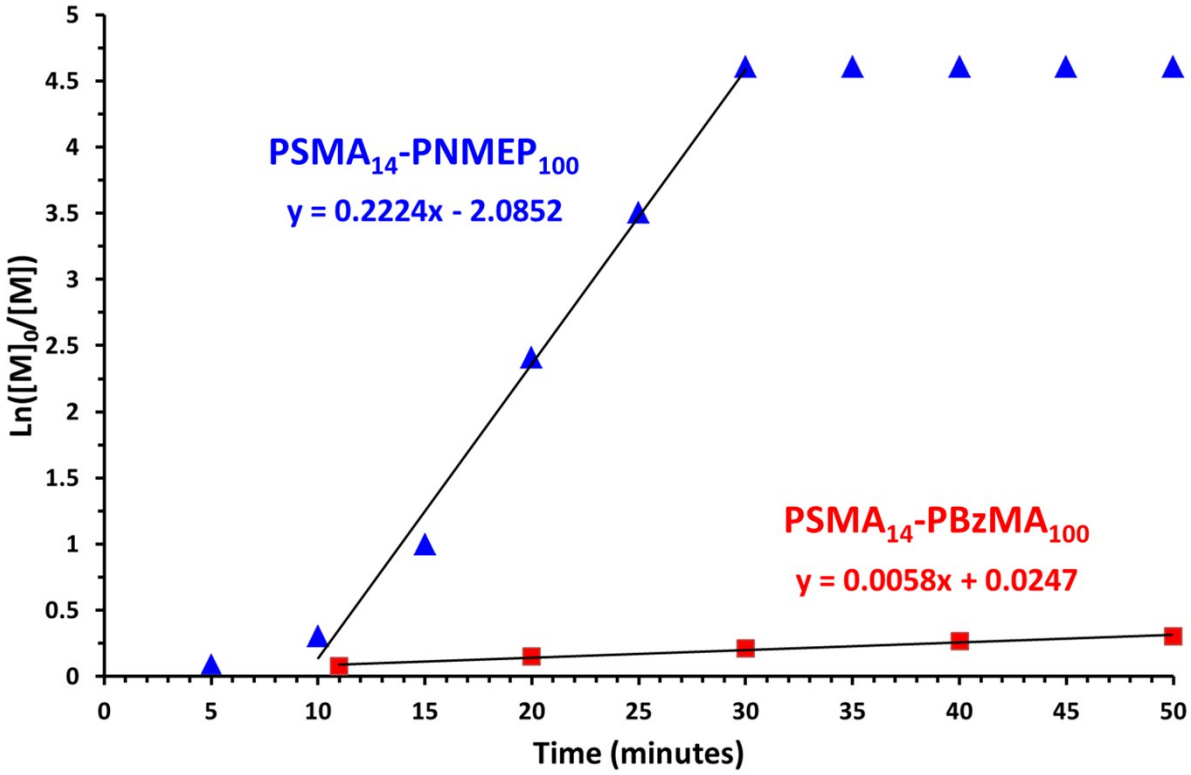


**Figure S3.** A plot of $Ln([M]_0/[M])$ against time for the kinetics of RAFT dispersion polymerisation of either NMEP or BzMA at 90°C when targeting either $PSMA_{14}$-$PNMEP_{100}$ (blue) or $PSMA_{14}$-$PBzMA_{100}$ (red), respectively. A short induction period is observed for the $PSMA_{14}$-$PNMEP_{100}$ formulation, but then the rate of this NMEP polymerisation proceeds with an apparent pseudo-first order rate constant that is 38 times greater than that of the BzMA polymerisation when targeting $PSMA_{14}$-$PBzMA_{100}$.

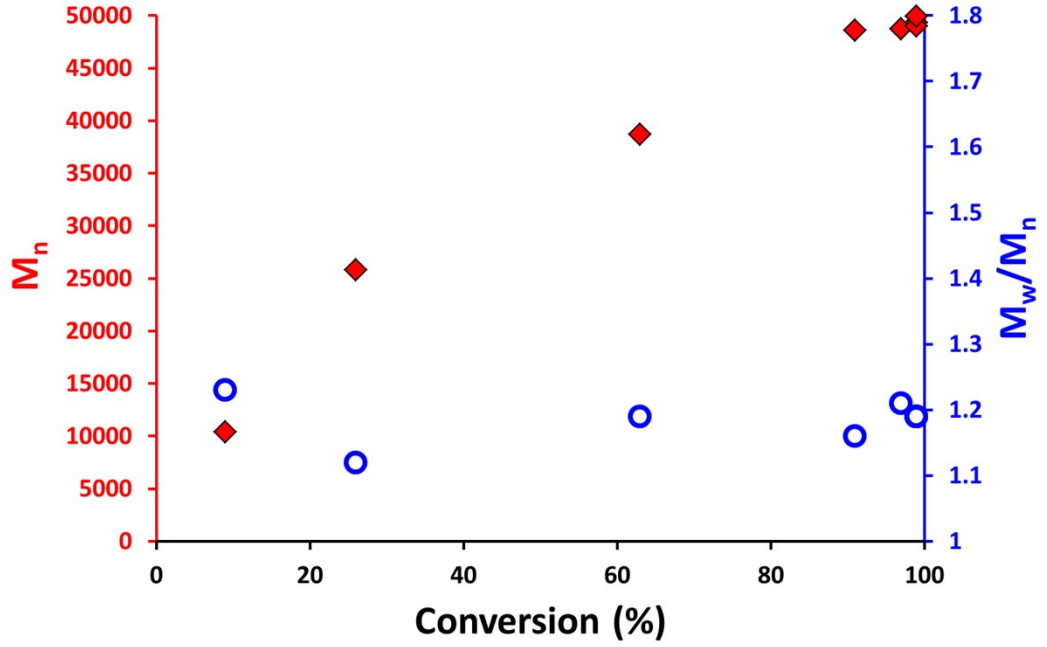


**Figure S4**. 3:1 Chloroform/methanol GPC data (versus a series of poly(methyl methacrylate) standards) obtained for the kinetics of polymerisation of NMEP when targeting $PSMA_{14}$-$PNMEP_{100}$

**Table S1.** Conversions, Molecular Weights ($M_n$), Polydispersities ($M_w/M_n$), DLS and TEM diameters obtained for $PSMA_{14}$-$PNMEP_x$ ($S_{14}$-$N_x$) Diblock Copolymer Nanoparticles prepared at 20% w/w Solids and the corresponding $PSMA_{14}$ Macro-CTA prepared at 40 % w/w Solids.

| | **Diblock Composition** | **Conversion[a] (%)** | **Solids content (% w/w)** | **3:1 v/v% chloroform methanol GPC** | | **Particle diameter** | **Particle morphology** |
|---|---|---|---|---|---|---|---|
| | | | | **$M_n$ [b] (kg mol$^{-1}$)** | **$M_w/M_n$ [b]** | **DLS[c] (nm)** | |
| S1 | $S_{14}$ | 80 | 40 | 7.5 | 1.12 | N/A | - |
| S2 | $S_{14}$-$N_{49}$ | 99 | 20 | 29.7 | 1.15 | 26 (0.049) | Spheres |
| S3 | $S_{14}$-$N_{79}$ | 99 | 20 | 44.5 | 1.22 | 36 (0.055) | Spheres |
| S4 | $S_{14}$-$N_{99}$ | 99 | 20 | 52.7 | 1.27 | 39 (0.054) | Spheres |
| S5 | $S_{14}$-$N_{114}$ | 95 | 20 | 63.3 | 1.34 | 48 (0.054) | Spheres |
| S6 | $S_{14}$-$N_{149}$ | 99 | 20 | 84.3 | 1.59 | 151 (0.093) | Mixed |
| S7 | $S_{14}$-$N_{173}$ | 99 | 20 | 85.0 | 1.48 | 1174 (0.324) | Mixed |
| S8 | $S_{14}$-$N_{190}$ | >99 | 20 | 89.8 | 1.75 | 824 (0.305) | Mixed |
| S9 | $S_{14}$-$N_{198}$ | 99 | 20 | 99.4 | 2.01 | 722 (0.348) | Worms |
| S10 | $S_{14}$-$N_{209}$ | 99 | 20 | 105.8 | 1.79 | 729 (0.461) | Mixed |
| S11 | $S_{14}$-$N_{221}$ | 98 | 20 | 111.5 | 1.94 | 1370 (0.302) | Mixed |
| S12 | $S_{14}$-$N_{248}$ | 99 | 20 | 121.9 | 2.04 | 1169 (0.115) | Mixed |

a. Monomer conversion determined by $^1$H NMR spectroscopy in $CDCl_3$.
b. Determined by 3:1 v/v chloroform/methanol GPC against poly(methyl methacrylate) calibration standards using a refractive index detector.
c. The numbers in brackets refer to the DLS polydispersity

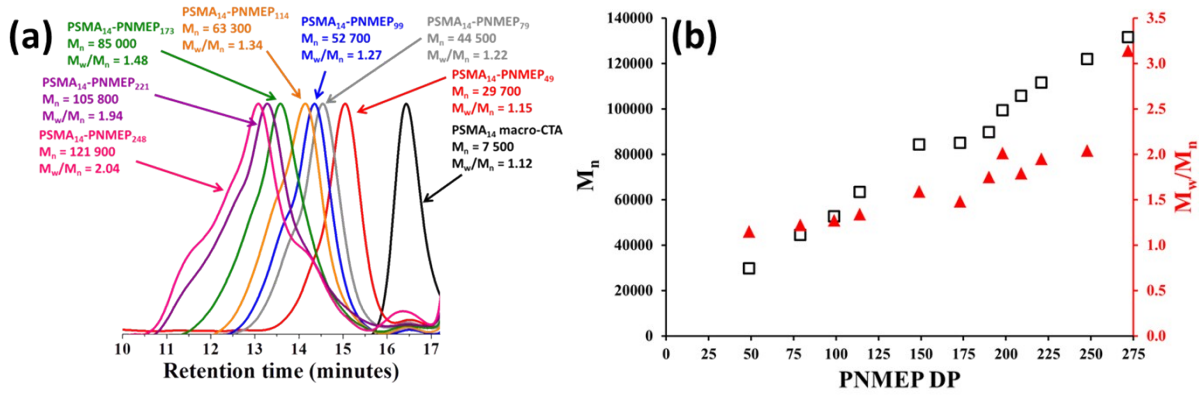


**Figure S5.** (a) 3:1 Chloroform/methanol GPC curves obtained for a selection of $PSMA_{14}$-$PNMEP_x$ diblock copolymer nanoparticles prepared at 20% w/w solids via RAFT dispersion polymerisation of NMEP at 90 °C. (b) A plot of $M_n$ (black axis) and $M_w/M_n$ (red axis) against PNMEP DP for the same series of $PSMA_{14}$-$PNMEP_x$ diblock copolymer nanoparticles.

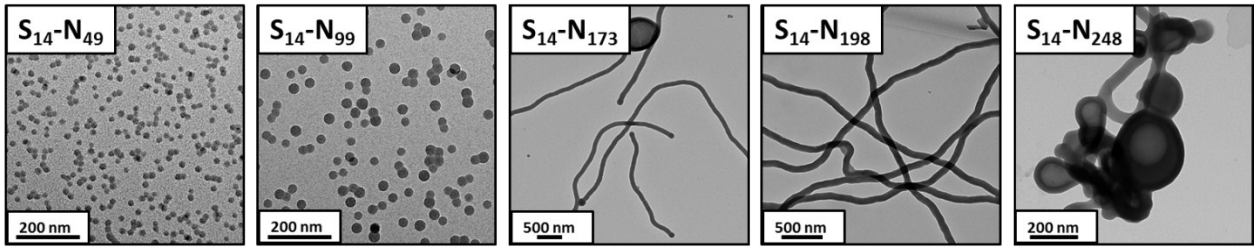


**Figure S6.** Representative TEM images obtained for $PSMA_{14}$-$PNMEP_x$ diblock copolymer nano-objects prepared via RAFT dispersion polymerisation of NMEP at 20% w/w solids.

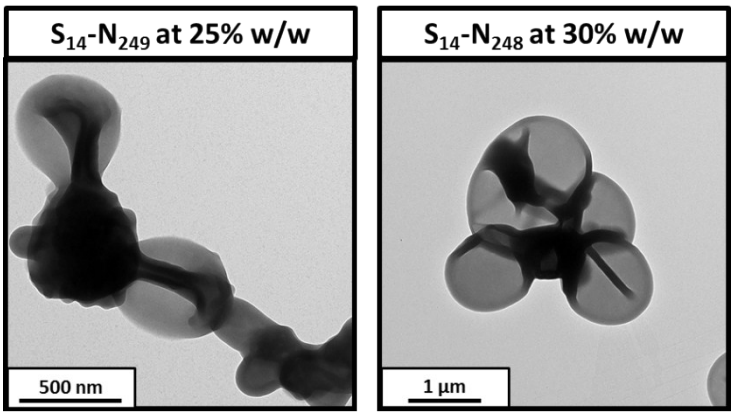


**Figure S7.** Representative TEM images recorded for the unstable precipitate phase obtained for $PSMA_{14}$-$PNMEP_x$ syntheses conducted at either 25% or 30% solids when targeting a PNMEP DP of 250.

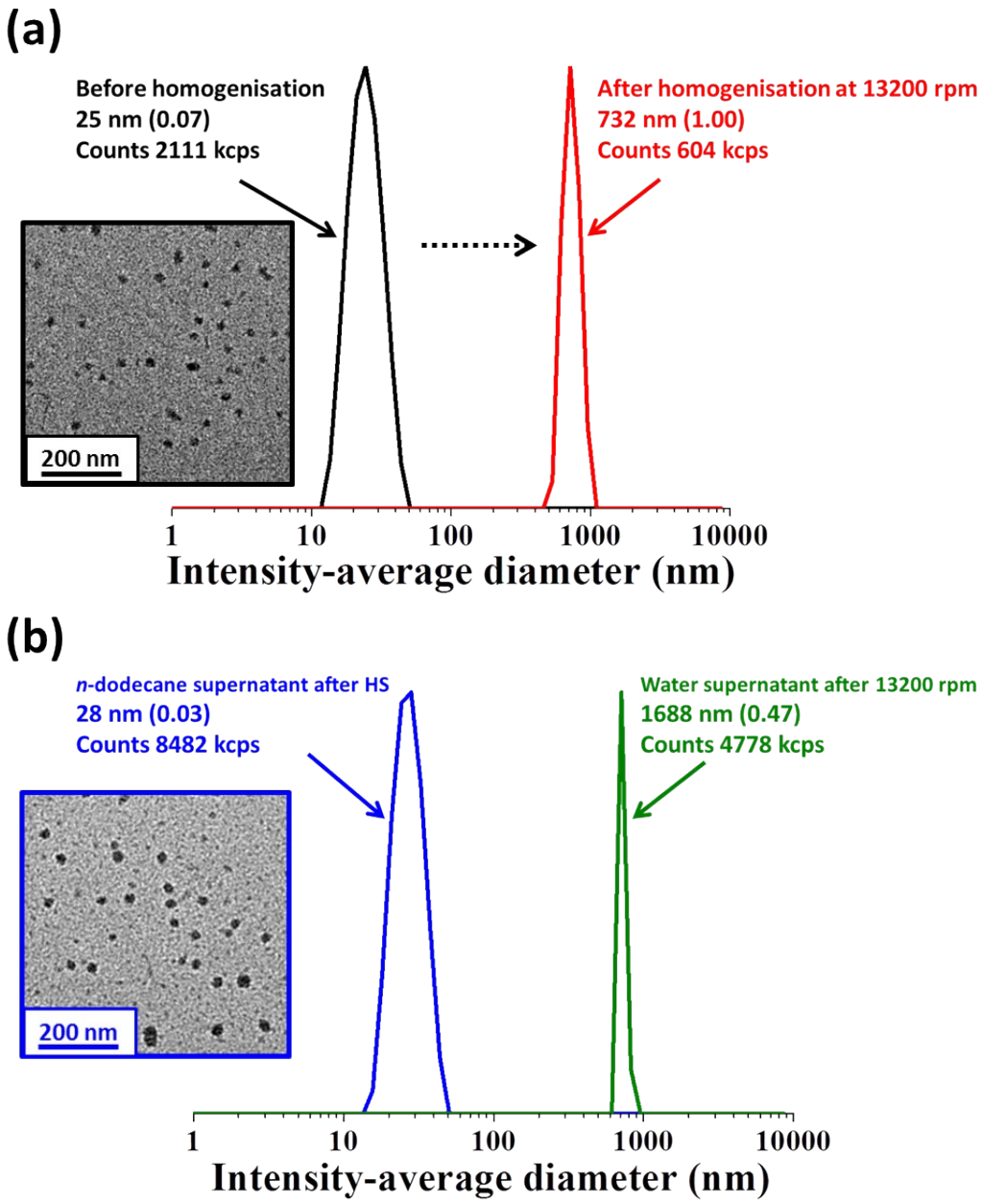


**Figure S8.** (a) DLS particle size distributions obtained at 25°C for $PSMA_{14}$-$PNMEP_{49}$ nanoparticles before (black) and after (red) homogenisation at 13,200 rpm at 20°C. High shear homogenisation causes the initial 25 nm spherical nanoparticles to break up, resulting in a relatively low count rate and a very high polydispersity. Inset: TEM image before homgenisation. (b) DLS particle size distributions obtained for the *supernatants* (after gravitational sedimentation of the aqueous droplet phase on standing at 20°C overnight) of water-in-oil emulsions prepared using 1.0% w/w $PSMA_{14}$-$PNMEP_{49}$ nanoparticles. The blue trace shows the DLS size distribution (and corresponding TEM image) obtained for the *n*-dodecane *supernatant* of the water-in-oil emulsion prepared by hand-shaking, confirming that these nanoparticles are stable to homogenisation at *low* shear (hand-shaking). The green trace shows the *aqueous* supernatant of the oil-in-water emulsion obtained after preparation via homogenisation at 13,200 rpm.

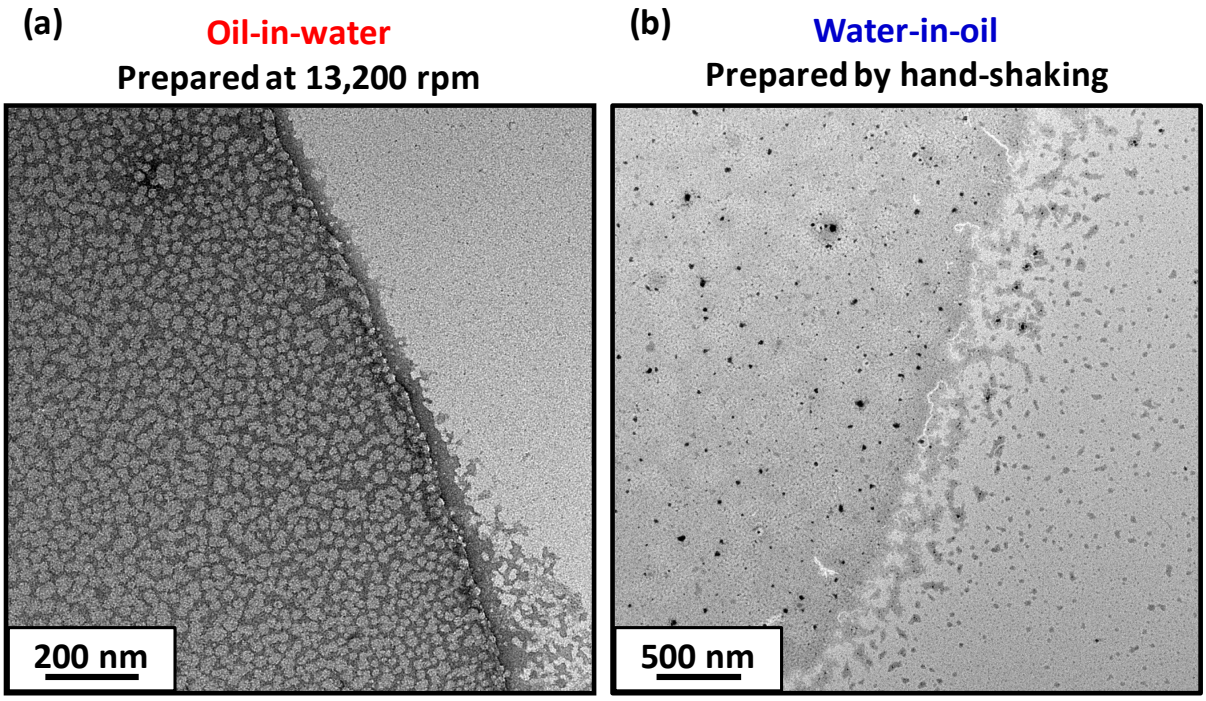


**Figure S9.** Transmission electron microscopy of Pickering emulsion droplets prepared using $PSMA_{14}$-$PNMEP_{49}$; (a) an oil-in-water droplet prepared at 13,200 rpm and stained using uranyl formate and (b) a water-in-oil droplet prepared by hand-shaking and stained using ruthenium(VIII) oxide. Both show the presence of spherical nanoparticles absorbing at the oil-water interface.

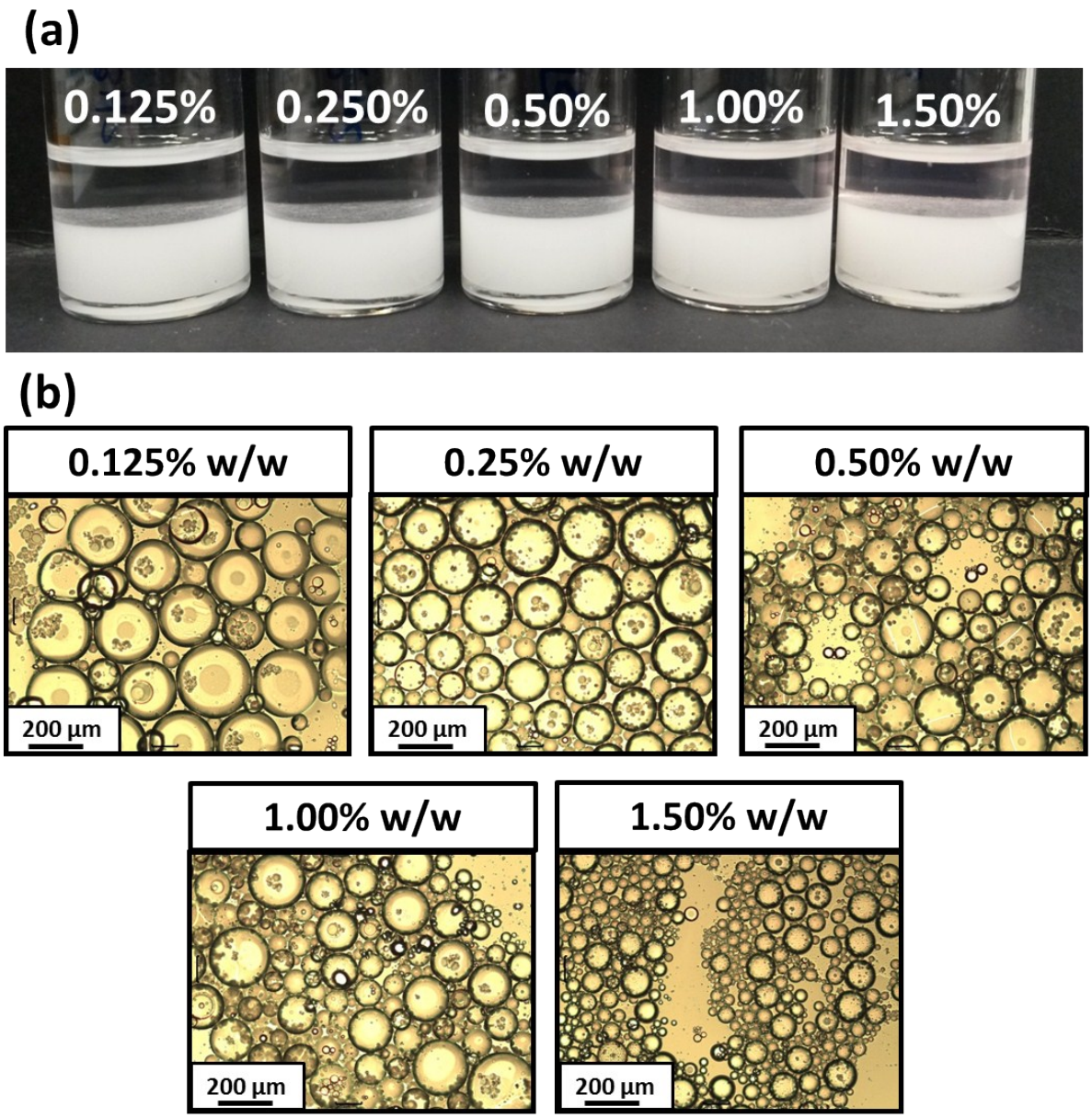


**Figure S10.** Water-in-oil emulsions prepared by hand-shaking of 50:50v/v mixtures of *n*-dodecane and water using either 0.125%, 0.25% 0.50%, 1.00% or 1.50% w/w $PSMA_{14}$-$PNMEP_{49}$ nanoparticles: (a) digital photograph of the resulting five emulsions and (b) corresponding optical microscopy images.

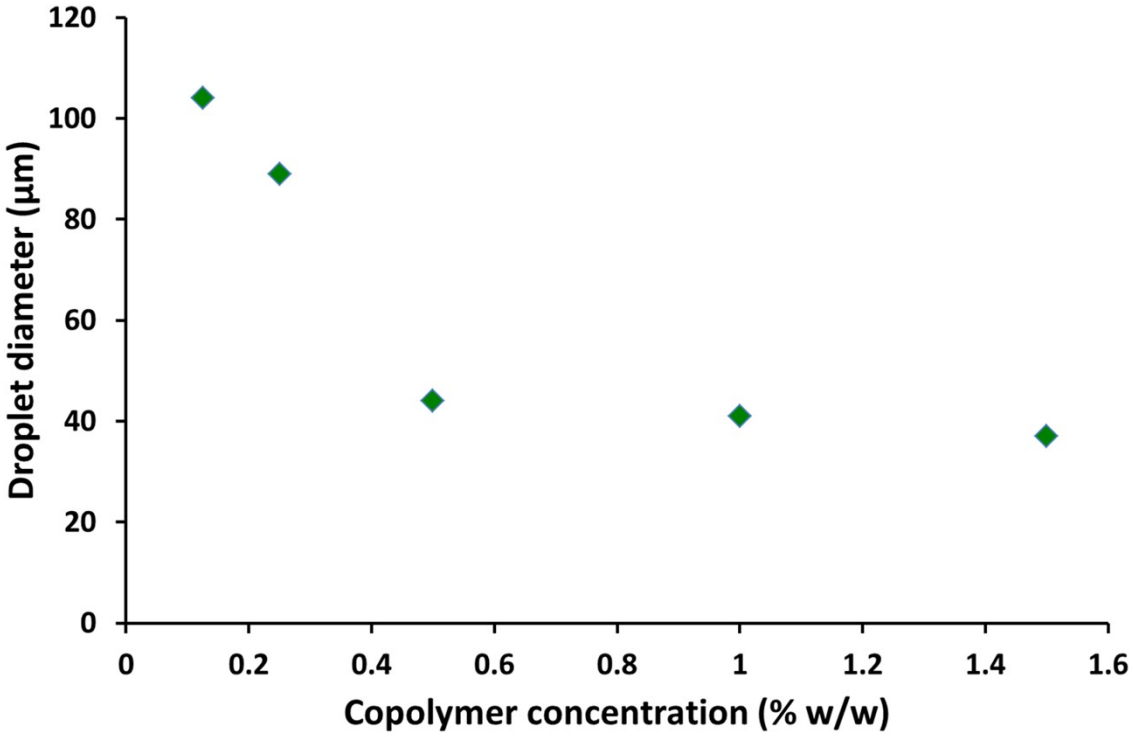


**Figure S11.** Concentration dependence of the mean aqueous droplet diameter obtained for the water-in-oil emulsions prepared by hand-shaking using either 0.125%, 0.25% 0.50%, 1.00% or 1.50% w/w $PSMA_{14}$-$PNMEP_{49}$ nanoparticles. Mean droplet diameters were estimated from optical microscopy images by analysing at least 100 droplets.

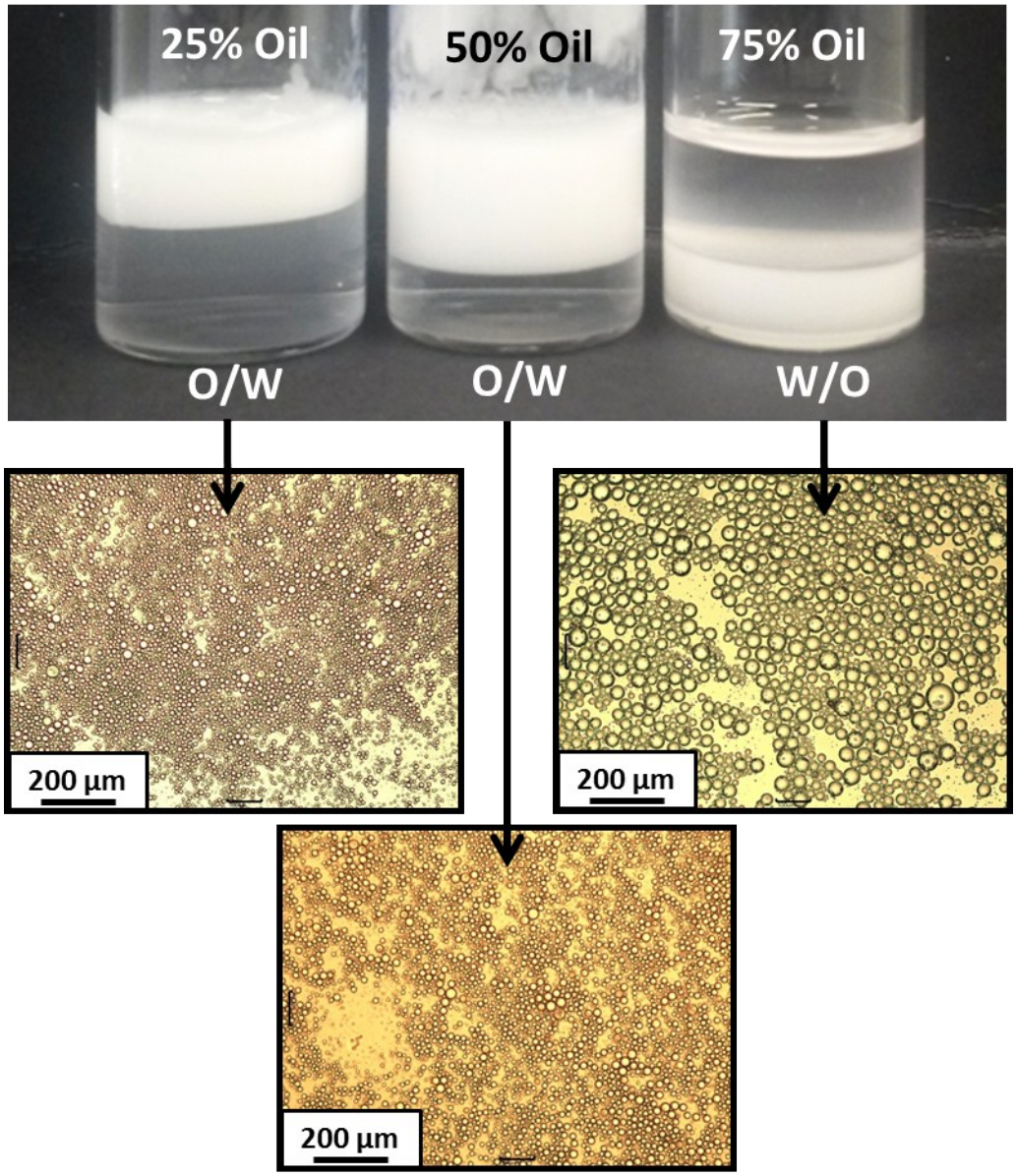


**Figure S12.** Digital photographs and corresponding optical microscopy images obtained for $PSMA_{14}$-$PNMEP_{49}$ emulsions formed using water volume fractions 0.25, 0.50 or 0.75 relative to *n*-dodecane. Emulsions were prepared using 0.5% w/w $PSMA_{14}$-$PNMEP_{49}$nanoparticles at 13,200 rpm. The latter water volume fractions resulted in the formation of *oil-in-water* emulsions, whereas the lowest water volume fraction produced a *water-in-oil* emulsion.